Two-photon interference : spatial aspects of two-photon entanglement, diffraction, and scattering

Peeters, W.H.

1 Introduction

1.1 Interference in optics

1.1.1 Young's experiment: interference of waves

Around 1801, the British scientist Thomas Young demonstrated that light propagates like a wave. Light waves, in contrast to light rays, can form interference patterns. Young illuminated a mask with two parallel slits with monochromatic spatially coherent light and projected the transmitted light onto a screen. He observed a periodic intensity pattern of bright and dark lines, which he explained as an interference pattern. Figure 1.1 illustrates a simulation of a wave passing through a mask with two slits. The two waves that emerge from the slits expand in a circular manner such that they cross each others path. In the low-intensity regions, the phases of the two waves are opposite, and the waves interfere destructively at any instant of time. In the high-intensity regions, both waves interfere constructively yielding a larger detected intensity.

Later, in 1865, James Clerk Maxwell theoretically showed that the electric field and the magnetic field, together, can form a wave that propagates at exactly the speed of light [1]. Ever since, light is understood as a wave of the electromagnetic field. Classically, the state of the electromagnetic field is determined by the electric field $\mathbf{E}(\mathbf{r}, t)$ and the magnetic field $\mathbf{B}(\mathbf{r}, t)$. The time evolution of these fields is described by Maxwell's equations. [2].

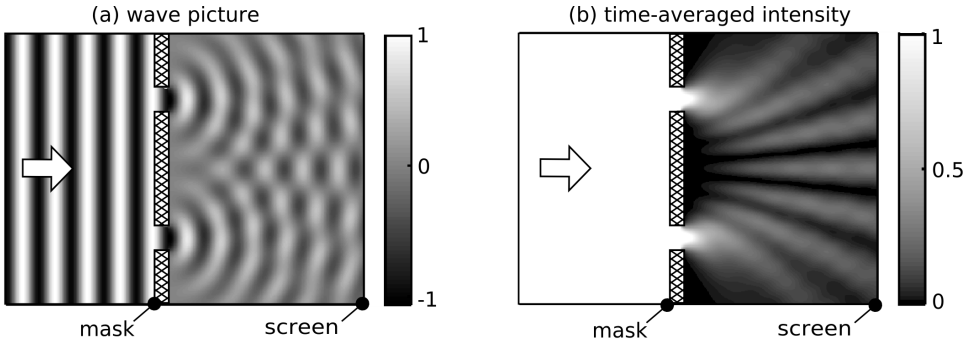

Figure 1.1: (a) Simulation of a wave propagating through a mask with two slits. The grey scale represents the wave displacement at some instant of time. (b) An interference pattern is formed in the time-averaged intensity profile behind the mask. Around 1801, Thomas Young demonstrated that light produces such intensity pattern. He visualized this interference pattern by projecting the transmitted light onto a screen.

1.1.2 One-photon and two-photon interference

The quantum theory of light describes the quantum state $|\Psi\rangle$ of the electromagnetic field [3,4]. Formally, this theory is obtained by applying a procedure called canonical quantization to the classical theory of the electromagnetic field. The foundation of multiphoton interference within quantum optics was laid by Glauber in 1963 in his influential work on quantum optical coherence [5]. The quantum theory replicates the occurrence of the classical interference patterns of the intensity similar to the one shown in Fig. 1.1(b). Additionally, Glauber's analysis makes clear that quantum interference can occur in n-fold intensity correlations between n separate detectors. This type of optical interference is now referred to as n-photon interference.

Young's classical interference pattern in Fig. 1.1 is a one-photon interference phenomenon. One-photon interference refers to a structure in the photon detection rate in a single detector. The photon detection rate is [5]

$$R^{(1)}(\mathbf{r},t) \propto \langle\Psi|\hat{E}^{-}(\mathbf{r},t)\hat{E}^{+}(\mathbf{r},t)|\Psi\rangle, \tag{1.1}$$

where $\hat{E}^{\pm}(\mathbf{r},t)$ are the positive and negative frequency electric-field operators at position $\mathbf{r}$ and time t. A one-photon interference pattern can in principle be formed by a single photon only. So if one would perform Young's experiment with a single photon, the probability of where the photon can be absorbed corresponds to the intensity pattern obtained from the classical wave theory [see Fig.1.1(b)].

Two-photon interference refers to a structure in the coincidence rate between

two detectors. Glauber argued that this coincidence rate is [5]

$$R^{(2)}(\mathbf{r}_1,t_1;\mathbf{r}_2,t_2) \propto \langle\Psi|\hat{E}^-(\mathbf{r}_1,t_1)\hat{E}^-(\mathbf{r}_2,t_2)\hat{E}^+(\mathbf{r}_2,t_2)\hat{E}^+(\mathbf{r}_1,t_1)|\Psi\rangle, \tag{1.2}$$

where $\mathbf{r}_{1,2}$ and $t_{1,2}$ are space and time coordinates of the two detectors. It may not be obvious from Eq. (1.2) how two-photon interference can occur. Let us therefore construct the two-photon state*

$$|\Psi\rangle = \frac{1}{\sqrt{2}}\int d\mathbf{k}_1 d\mathbf{k}_2\ \phi^{(2)}(\mathbf{k}_1,\mathbf{k}_2)\hat{a}^\dagger(\mathbf{k}_1)\hat{a}^\dagger(\mathbf{k}_2)|\text{vac}\rangle, \tag{1.3}$$

where $\phi^{(2)}(\mathbf{k}_1,\mathbf{k}_2) = \phi^{(2)}(\mathbf{k}_2,\mathbf{k}_1)$ without loss of generality, $|\text{vac}\rangle$ is the continuous-mode vacuum, and $\hat{a}^\dagger(\mathbf{k})$ is the continuous-mode photon creation operator with momentum $\mathbf{k}$. For our interest in simplicity, we have restricted ourselves to one polarization only. Let us also specialize to paraxial light where $\phi^{(2)}(\mathbf{k}_1,\mathbf{k}_2)$ is nonzero only for $\mathbf{k}$ vectors that are oriented paraxially. By combining Eqs. (1.2) and (1.3), we find the two-photon interference pattern†

$$\begin{aligned} R^{(2)}(\mathbf{r}_1,t_1;\mathbf{r}_2,t_2) \quad \propto \quad & \Bigg| \int d\mathbf{k}_1 d\mathbf{k}_2\ \phi^{(2)}(\mathbf{k}_1,\mathbf{k}_2) \exp\left(i\mathbf{k}_1\cdot\mathbf{r}_1 - i|\mathbf{k}_1|ct_1\right) \\ & \times \exp\left(i\mathbf{k}_2\cdot\mathbf{r}_2 - i|\mathbf{k}_2|ct_2\right) \Bigg|^2, \end{aligned} \tag{1.4}$$

where c is the speed of light. The absolute square operation directly reveals the interference mechanism behind two-photon interference. The expression between $|..|^2$ is the two-photon wave packet, which is a complex (rotating) amplitude as a function of two coordinates. Each coordinate is propagated according to the scalar wave equation of light.

Two-photon interference is especially interesting if the two photons in Eq. (1.3) are entangled. In the entangled case, the two-photon amplitude does not factorize in two functions‡, i.e.,

$$\phi^{(2)}(\mathbf{k}_1,\mathbf{k}_2) \neq f(\mathbf{k}_1)f(\mathbf{k}_2).$$

---

* We use the continuous-mode formalism with usual commutation relations and field operators given by Eqs. (10.10-1)-(10.10-4) in Ref. [3]. Normalization then corresponds to $\int d\mathbf{k}_1 d\mathbf{k}_2 |\phi^{(2)}(\mathbf{k}_1,\mathbf{k}_2)|^2 = 1$, where we have imposed $\phi^{(2)}(\mathbf{k}_1,\mathbf{k}_2) = \phi^{(2)}(\mathbf{k}_2,\mathbf{k}_1)$ without loss of generality since any asymmetry drops out of Eq. (1.3).

† We adjusted the electric-field operator in Eq. (1.2) to a similar operator related to the square root of the photon density (the continuous-mode version of equation (12.3-1) in Ref. [3]). The expression for this adjusted field operator (in single-polarization form) is $\hat{V}^+(\mathbf{r},t) = \sqrt{(2\pi)^{-3}}\int d\mathbf{k}\ \hat{a}(\mathbf{k})\exp[i\mathbf{k}\cdot\mathbf{r} - i|\mathbf{k}|ct]$.

‡ It is debatable whether inseparability also implies entanglement. For example: is it correct to call $\phi^{(2)}(\mathbf{k}_1,\mathbf{k}_2) = f(\mathbf{k}_1)g(\mathbf{k}_2) + f(\mathbf{k}_2)g(\mathbf{k}_1)$ entangled? We will refer to this two-mode form of inseparability as entanglement between indistinguishable photons (see chapter 4).

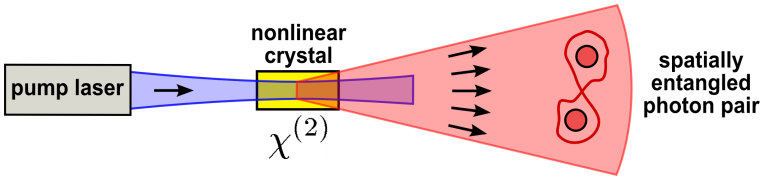

Figure 1.2: Experimental geometry for the operation of spontaneous parametric down-conversion. The down-converted light is spatially multimode (indicated by the arrows). Each down-converted photon pair is spatially entangled due to conservation of transverse momentum in the down-conversion process.

If this function would factorize, the two-photon interference pattern would become a trivial multiplication of the one-photon interference patterns, i.e.,

$$R^{(2)}(\mathbf{r}_1, t_1; \mathbf{r}_2, t_2) \propto R^{(1)}(\mathbf{r}_1, t_1) R^{(1)}(\mathbf{r}_2, t_2) \qquad [\text{if } \phi^{(2)}(\mathbf{k}_1, \mathbf{k}_2) \text{ factorizes}].$$

If the two-photon amplitude does not factorize, the one-photon interference pattern generally gets washed out, but, at the same time, the two-photon interference pattern retains its high visibility. Two-photon interference occurs most prominently in a two-photon state. The presence of a three-photon component (or more photons) will lower the visibility of the two-photon interference pattern if $\phi^{(2)}(\mathbf{k}_1, \mathbf{k}_2)$ is not factorizable. Therefore, one requires two-photon states to study interesting two-photon interference phenomena with high visibility.

1.1.3 Spontaneous parametric down-conversion: a source of pairs of entangled photons

Nowadays, two-photon interference experiments are commonly performed with photon pairs produced by the nonlinear $\chi^{(2)}$ process of spontaneous parametric down-conversion (SPDC). The process is operated by directing a coherent pump laser through a nonlinear crystal (see Fig. 1.2). SPDC refers to the occasional spontaneous splitting of a pump photon into two photons of lower energy (see Sec. 1.3 for details). These photon pairs can be observed as simultaneous clicks by two single photon detectors, as was first observed in 1970 [6]. Most interestingly, the photons within a pair are spatially entangled resulting from the conservation of transverse momentum in the down-conversion process. Loosely speaking, each photon is incoherently emitted in many spatial modes, but, at the same time, the pair as a whole is pure and has the well defined transverse momentum distribution of the pump beam. Section 1.3 describes how the down-converted stream of photon pairs can be identified with a two-photon wave packet similar to Eq. (1.3). The photon pairs produced by SPDC are thus excellent candidates for the research on two-photon

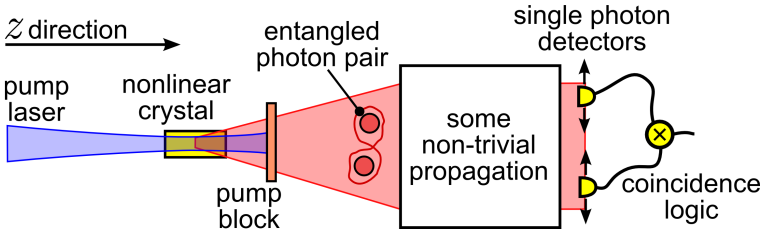

Figure 1.3: Generic scheme of the two-photon interference experiments discussed in this thesis. Two-photon interference phenomena are experimentally observed via the coincidence count rate in the plane of the detectors.

interference. Two-photon interference was first observed in 1987 by Ghosh, Hong, Ou, and Mandel [7, 8].

1.2 Research topics in this theses

1.2.1 Two-photon interference: three themes

The research in this thesis addresses spatial aspects of two-photon interference. The work is mainly experimental although our experiments are supported by theoretical models. The research can be divided into three research themes: We address (1) orbital angular momentum entanglement, (2) two-photon diffraction from a double slit, and (3) two-photon scattering of a random medium.

Despite their diversity, all themes are strongly related to one another. This is because two-photon interference and spatial entanglement play dominant roles in all themes. A generic scheme of all interference experiments is displayed in Fig. 1.3. Pairs of spatially entangled photons are emitted by the SPDC source and propagate through the experimental setup before being detected by two single-photon detectors. The propagation part is different for each experiment depending on the addressed research theme. Figure 1.4 illustrates the three setups that correspond to the three research themes. These research themes are discussed below in Secs. 1.2.2-1.2.4.

1.2.2 Theme 1: Orbital angular momentum entanglement

The spatial entanglement in the down-converted photon pair is of a high-dimensional form [9, 10]. This aspect is attracting a lot of attention because of its potential applicability in the field of quantum information processing [11–14]. The best studied basis of the spatial entanglement involves the orbital angular momentum (OAM) eigenstates [15–19]. If one photon is detected with OAM $+\hbar l$ then the other photon

must collapse into a spatial profile with $-\hbar l$. This is because the pump beam is just a Gaussian $l = 0$ beam, and OAM is conserved in the down-conversion process. The quantum state of the photon pair can thus be tentatively written as*

$$|\Psi\rangle \sim \sum_{l=-\infty}^{\infty} \sqrt{P_l} \big| + l\hbar \big\rangle_1 \otimes \big| - l\hbar \big\rangle_2 \qquad \text{[omitting radial properties]},$$

where the probabilities $P_l = P_{-l}$ correspond to the distribution over the orbital angular momentum spectrum.

The distribution of the P_l coefficients can, in principle, be determined from the incoherent OAM distribution of just one of the photons [20, 21]. Such a measurement does, however, not depend on whether the photons are really entangled or not. The photons could equally well be a pair of independent incoherent photons with some OAM spectrum. In the literature, it was argued that the OAM distribution could also be determined via two-photon interference involving *both* entangled photons [22]. The experimental technique for this experiment is illustrated in Fig. 1.4 (theme 1). The orbital-angular momentum spectrum is contained in the visibility of the multimode Hong-Ou-Mandel dip as a function of the rotation angle of the image rotator [22]. In this thesis, we have used this challenging technique to determine the OAM distribution of the entangled photons. We also consider several special cases and provide a more detailed theoretical analysis supporting the experiment.

1.2.3 Theme 2: Two-photon diffraction from a double slit

Starting from 1994, a lot of experiments have addressed two-photon diffraction from a double-slit [23–35]. So why would one still want to study this topic? The reason is that the diversity of possible two-photon interference patterns behind a double slit has, we believe, not been widely appreciated. In fact, most of the possible forms of spatial entanglement behind the double slit have remained unexplored so far.

The most general two-photon state behind the double-slit (under symmetric two-photon illumination) can be written as

$$|\Psi\rangle = \cos(\alpha/2) \left(\frac{|\uparrow\downarrow\rangle + |\downarrow\uparrow\rangle}{\sqrt{2}} \right) + e^{i\varphi} \sin(\alpha/2) \left(\frac{|\uparrow\uparrow\rangle + |\downarrow\downarrow\rangle}{\sqrt{2}} \right), \tag{1.5}$$

where $|\uparrow\rangle$ and $|\downarrow\rangle$ represent transmissions through the top and bottom slit, and parameters α and φ determine the quantum state. This state can be recognized as a superposition of two maximally entangled Bell states. The first Bell state corresponds to photons going through opposite slits; the second term corresponds to

* The full Schmidt decomposition also involves the radial properties of the mode profiles (see Ref. [9] and chapter 2): $|\Psi\rangle = \sum_{l=-\infty}^{\infty} \sum_{p=0}^{\infty} \sqrt{P_{l,p}}\, |l\hbar, p\rangle_1 \otimes |-l\hbar, p\rangle_2$.

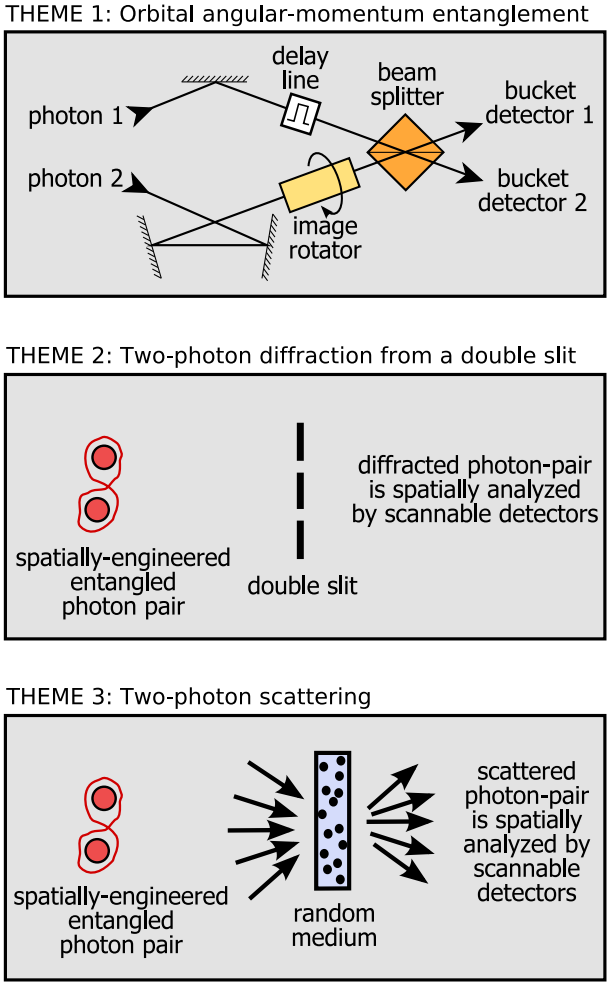

Figure 1.4: Three themes addressing two-photon interference in this thesis. The illustrations represent the propagation-boxes that can be inserted into Fig. 1.3.

photons choosing the same slit. So far, no attention has been paid to the experimental tuning of the phase φ. However, this phase is extremely important for the degree and type of entanglement. One could, for example, consider the maximally entangled state at $\alpha = \varphi = \frac{1}{2}\pi$. In this form of entanglement, the path of photon 1 is quantum correlated with the state $|\uparrow\rangle \pm i|\downarrow\rangle$ of photon 2, while path-path correlation is absent.

In comparison to other experiments on the two-photon double slit, our research is novel in three different ways. First, we demonstrate how to engineer the spatial entanglement with full control over state parameters α and φ. Secondly, our analysis provides a deeper understanding of the spatial structure in the entanglement between down-converted photons. We address, for the first time, phase-sensitive aspects of the two-photon field in the near-field of the generating crystal. Finally, we measure entire two-photon diffraction patterns in the far-field of the double slit with unprecedented quality. Our experiments reveal, in a very pure manner (namely: double-slit diffraction), the large diversity of two-photon interference patterns.

1.2.4 Theme 3: Two-photon scattering

This theme is the most advanced. Until now, the propagation of entangled photon pairs through a random medium has never been investigated experimentally. Only recently, a few theoretical papers have appeared [36–38]. Why would one want to study such a topic? The reason is simple. One-photon interference effects in random media are widely studied and have proven to be extremely interesting and diverse [39, 40]. Interesting phenomena within one-photon scattering are speckle [41], enhanced backscattering [42, 43], universal conductance fluctuations [44], and Anderson localization of light [43, 45–47]. Can we discover similar phenomena for two-photon interference in the case of two-photon scattering?

There are thus enough interesting questions to ask about two-photon scattering. How does two-photon speckle look like? How does scattering affect the entanglement between the photons? In which way does the scattered two-photon state contain information about the scattering medium? Do there exist two-photon interference phenomena that survive averaging over different realizations of disorder? In this thesis, all the above questions are, to a large extent, answered and experimentally demonstrated.

1.3 Quantum description of SPDC light

1.3.1 Motivation

In the previous section, we presented an overview of the topics that are investigated in this thesis. Despite the diversity, all experiments address the same observable: the time-averaged coincidence count rate in continuous-wave (cw) pumped, low-gain* SPDC light. For each experiment, we have made a theoretical model providing a solid understanding of the experimental results. All models are based on a quantum description of SPDC light. More specifically, the models are based on a single concept called the two-photon field. As the two-photon field plays a central role in this thesis, we have devoted Secs. 1.3.2-1.3.5 to a discussion of the theoretical foundation of this concept.

1.3.2 Two approaches to describe SPDC light

The description of SPDC light requires a quantum-mechanical treatment of the SPDC process†. There is a substantial amount of literature on the theory of SPDC [3,4,49,51–65]. The treatments can be divided into two categories depending on the approach.

The first approach uses the quantized version of the input-output relations of a parametric amplifier [3, 4, 49, 60–62, 64]. The light in the output channels is described as a noisy signals exhibiting quantum Gaussian noise [49,58]. This approach is suitable for both the low-gain and high-gain regime of SPDC and has gained popularity in the last decade [50, 60, 62, 64, 66]. Most papers just analyse a two-channel parametric amplifier (signal and idler), although spatially multimode SPDC has also been treated in this way [60, 61, 67].

The second approach is based on a first-order perturbative analysis of the time-evolution operator [3, 51, 53–55, 57, 59, 63, 65, 68]. This approach only works in the low-gain regime since a first-order perturbation analysis yields at most a single photon pair. All spatial and temporal correlations between the photons are contained in the resulting quantum state. As all experiments in this thesis are performed in

* Parametric gain corresponds to the strength at which the signal and idler fields are amplified due to parametric interaction with the strong pump beam. Low gain means that a generated photon pair has low probability ($\ll 1$) to stimulate the generation of another pair (thus creating four photons) during transmission through the crystal.

† Other $\chi^{(2)}$ processes like second harmonic generation and sum/difference frequency generation can be understood classically. These processes can be described as radiation emitted by a classically oscillating polarization of the nonlinear medium. This is not possible for the SPDC process. Besides, high-visibility two-photon interference phenomena can not be understood classically either. One can, in theory at least, construct classical signals that exhibit some form of two-photon interference with a strongly reduced visibility. The maximum visibility that can be constructed classically is a rather complicated issue [48–50].

the low-gain regime, we use a description of the SPDC light that is based on the perturbative approach (see Sec. 1.3.3).

1.3.3 Two-photon field

Based on the perturbative approach, the concept of the two-photon field was put forward in Refs. [54, 56] by Rubin, Klyshko, Shih, and Sergienko. In the first-order perturbation method, the quantum state of the generated SPDC light is calculated as [3, 53–55, 59, 65, 68]

$$|\Psi(\tau)\rangle \approx |\mathrm{vac}\rangle - \frac{i}{\hbar}\int_0^\tau dt\ \hat{H}_I(t)|\mathrm{vac},\rangle \tag{1.6}$$

where τ is the interaction time, and $\hat{H}_I(t)$ is the interaction Hamiltonian of the $\chi^{(2)}$ nonlinear process driven by a classical, paraxial, and monochromatic pump beam $E(\mathbf{r}, t)$ [3, 53, 59]. The interaction Hamiltonian contains two photon creation operators and depends linearly on the driving field of the pump beam, the interaction volume, and the second-order nonlinear susceptibility $\chi^{(2)}$ of the crystal.

The second term in Eq. (1.6) is a two-photon component. The norm of this component grows linearly with the interaction time*. Intuitively, state $|\Psi(\tau)\rangle$ is only experimentally meaningful if the norm of the two-photon component stays way below unity even for interaction times τ much greater than the transmission time through the crystal (which implies the low-gain regime). Then, the interaction time for which this norm equals unity corresponds to the average time between successive down-conversions†. The quantum state $|\Psi(\tau)\rangle$ contains all spatial and temporal correlations between the down-converted photons and is thus effective in describing multimode two-photon interference experiments [51, 68, 69].

The normalization of $|\Psi(\tau)\rangle$ breaks down dramatically for large interaction times [3]. Nonetheless, this normalization issue is often ignored in the literature; in many papers, the interaction time is simply taken to infinite yielding [54,57,59,63,68]

$$|\Psi_\infty\rangle \equiv |\mathrm{vac}\rangle - \frac{i}{\hbar}\int_{-\infty}^{\infty} dt\ \hat{H}_I(t)|\mathrm{vac}\rangle. \tag{1.7}$$

The normalizability of $|\Psi_\infty\rangle$ breaks down on account of the first-order perturbation method, the infinite interaction time, and the infinite duration of the driving cw pump beam (thus $\langle\Psi_\infty|\Psi_\infty\rangle = \infty$). Quite remarkably, this normalization issue is hardly ever discussed; it is, to the best of our knowledge, only addressed by

* See equations (22.4-23) to (22.4-25) in Ref. [3].
† Compare equations (22.4-25) and (22.4-31) in Ref. [3].

Shapiro *et al.* in Refs. [50, 62]. Mathematically, the state $|\Psi_\infty\rangle$ contains only two photons. In the laboratory, however, a typical SPDC source produces millions of photon pairs per second.

The two-photon field is defined as [54, 56]

$$A(\mathbf{x}_1, t_1, \mathbf{x}_2, t_2; z) \equiv \langle \mathrm{vac}|\hat{E}^+(\mathbf{x}_2, t_2; z)\hat{E}^+(\mathbf{x}_1, t_1; z)|\Psi_\infty\rangle, \tag{1.8}$$

where $\hat{E}^+(\mathbf{x}, t; z)$ is the positive frequency electric-field operator at transverse position $\mathbf{x}$, time t, and longitudinal position z. In the paraxial and narrow-band regime ($\Delta\omega \ll \omega$), the electric field operators can be expressed* in units of $\sqrt{\text{photons/m}^2\text{s}}$. The two-photon field then acquires units $(\text{m}^2\text{s})^{-1}$. The divergence of $|\Psi_\infty\rangle$ is also present in the two-photon field in a sense that it is not square integrable over all positions $\mathbf{x}_{1,2}$ and times $t_{1,2}$. The reason is that the two-photon field stretches out over an infinite amount of time. Nevertheless, its square amplitude in the time domain is finite and relates to the photon flux [54, 55, 62]. The two-photon field should thus be regarded as an unnormalizable two-photon wave packet† for which its amplitude in the time domain is related to the photon flux.

Based on Refs. [54, 56], the time-averaged coincidence count rate between two detectors at transverse positions $\mathbf{x}_1$ and $\mathbf{x}_2$ becomes

$$R_{\mathrm{cc}}(\mathbf{x}_1, \mathbf{x}_2; z) \propto \left(\frac{1}{2}\times\right) \int_{A_1} d^2\mathbf{x}_1' \int_{A_2} d^2\mathbf{x}_2' \int_{-\frac{1}{2}\tau_g}^{+\frac{1}{2}\tau_g} dt' \Big| A(\mathbf{x}_1 + \mathbf{x}_1', t, \mathbf{x}_2 + \mathbf{x}_2', t + t'; z)\Big|^2, \tag{1.9}$$

where $A_{1,2}$ are the transverse integration areas of the two detectors and τ_g is the gating time window of the coincidence logic. In typical experiments, the gate time τ_g is much larger than the spread in arrival times of the photons. Therefore, the integral over dt' can be taken over an infinite interval without changing the outcome of the integral. The factor $\frac{1}{2}$ between parentheses applies to type-I SPDC and is absent in type-II SPDC. This is because in type-I SPDC, the electric field operators in Eq. (1.8) have the same polarization and sense *both* photons in the two-photon state. In type-II SPDC, the electric field operators in Eq. (1.8) are assumed to have orthogonal polarizations and individually address only *one* of the photons, which are now distinguishable instead of indistinguishable. The square absolute value operation in Eq. (1.9) directly reveals the two-photon interference mechanism.

---

* The expression for the electric-field operator in units of square-root photon flux is $\hat{E}^+(\mathbf{r}, t) = \sqrt{c/(2\pi)^3}\int d\mathbf{k}\ \hat{a}(\mathbf{k}) \exp[i\mathbf{k}\cdot\mathbf{r} - i|\mathbf{k}|ct]$.

† For type-I SPDC, the identification with the symmetrized paraxial two-photon amplitude $\phi^{(2)}(\mathbf{k}_1, \mathbf{k}_2)$ in Eq. (1.3) becomes:
$A(\mathbf{r}_1, t_1, \mathbf{r}_2, t_2) = \frac{c\sqrt{2}}{(2\pi)^3}\int d\mathbf{k}_1 d\mathbf{k}_2\ \phi^{(2)}(\mathbf{k}_1, \mathbf{k}_2) \exp\left[i\mathbf{k}_1\cdot\mathbf{r}_1 + i\mathbf{k}_2\cdot\mathbf{r}_2 - i|\mathbf{k}_1|ct_1 - i|\mathbf{k}_2|ct_2\right]$.

Spatial propagation of the two-photon field from $z = 0$ to $z = z_d$ is described by applying the Maxwell electric-field propagators to each of the electric-field operators in Eq. (1.8). Naturally, spatial propagation is written down after a temporal Fourier transform, i.e,

$$A(\mathbf{x}_1, \omega_1, \mathbf{x}_2, \omega_2; z_d) = \int d^2\mathbf{x}_1' d^2\mathbf{x}_2' \; h(\mathbf{x}_1, z_d, \mathbf{x}_1', 0; \omega_1) h(\mathbf{x}_2, z_d, \mathbf{x}_2', 0; \omega_2) \times A(\mathbf{x}_1', \omega_1, \mathbf{x}_2', \omega_2; 0), \tag{1.10}$$

where $h(\mathbf{x}_f, z_f, \mathbf{x}_i, z_i; \omega)$ is the electric field propagator for any forward-propagating frequency-conserving optical system (see for example Ref. [70]). In principle, with the tools presented in this section, one can describe any low-gain two-photon interference experiment in the form of Fig. 1.3.

The absence of an equality sign in Eq. (1.9) is rather unfortunate. Although Rubin *et al.* [54,56] actually use an equality sign there, they state that their equation "defines" rather than calculates the coincidence count rate [54]. From our point of view, an analysis of the relationship between the photon flux and the unnormalizable two-photon state $|\Psi_\infty\rangle$ is not clearly present in the literature*. We conjecture, however, that the proportionality sign can be replaced by an equality sign (assuming high detection efficiency). Our argument is that if one would plug in a *normalized* paraxial two-photon state in Eq. (1.8), one would precisely get a single coincidence count when integrating $\left(\frac{1}{2}\times\right)|A(\mathbf{x}_1, t_1, \mathbf{x}_2, t_2; z)|^2$ over coordinates $\mathbf{x}_{1,2}$ and $t_{1,2}$. The norm of $|\Psi(\tau)\rangle$ in Eq. (1.6) can be interpreted as the expected number of photon down-conversions and grows linearly with interaction time τ. Therefore, it seems reasonable to assume that the proportionality sign in Eq. (1.9) can be replaced by an equality sign.

1.3.4 Expression for the two-photon field

Based on the treatments in Refs. [51, 69], and assuming the crystal to be infinitely wide in both transverse directions, the Fourier-transformed two-photon field of Eq. (1.8) is

$$A(\mathbf{q}_1, \omega_1, \mathbf{q}_2, \omega_2; 0) \propto \delta[\omega_p - (\omega_1 + \omega_2)] E_p(\mathbf{q}_1 + \mathbf{q}_2; z = 0) \times \mathrm{sinc}\left[\frac{L}{2}\Delta k_z(\mathbf{q}_1, \omega_1, \mathbf{q}_2, \omega_2)\right], \tag{1.11}$$

where $\delta(\omega)$ is the Dirac-delta function, $\mathrm{sinc}(x) \equiv \sin(x)/x$, $\mathbf{q}_{1,2}$ are transverse momenta of the two-photon field, ω_p is the angular frequency of the pump beam, L is the crystal length, and $E_p(\mathbf{q}; z = 0)$ is the complex amplitude of the cw pump

* Wong *et al.* [62] get rather close, although, eventually, a quantitative comparison between $|\Psi_\infty\rangle$ and their quantum Gaussian noise description is absent.

beam in momentum representation (in the crystal-center plane). The function

$$\Delta k_z(\mathbf{q}_1, \omega_1, \mathbf{q}_2, \omega_2) \equiv k_z(\mathbf{q}_1 + \mathbf{q}_2, \omega_p) - k_z(\mathbf{q}_1, \omega_1) - k_z(\mathbf{q}_2, \omega_2), \tag{1.12}$$

is the wave vector mismatch along the z direction of the crystal. Here, $k_z(\mathbf{q}, \omega)$ is the z component of the wave vector of a plane wave inside the crystal with transverse momentum $\mathbf{q}$ and angular frequency ω. The proportionality in Eq. (1.11) contains a linear dependence on the effective nonlinearity and the length of the crystal. The two-photon field in Eq. (1.11) contains all you need to know to describe spatial and temporal effects in two-photon interference experiments. It is also very general as it applies to all cw-pumped, low-gain SPDC processes in any kind of phase-matching geometry: type-I (same polarization), type-II (different polarizations), and quasi phase matching*.

Let us discuss some properties of the generated two-photon field in Eq. (1.11). First, the delta function $\delta[\omega_p - (\omega_1 + \omega_2)]$ ensures conservation of energy of the down-converted photons. The delta function also demonstrates that the two-photon field is unnormalizable since it spreads out infinitely long in the time domain. Secondly, the spread in the total transverse momentum of the down-converted photon pair is limited by the spread in momentum of the incident beam $E(\mathbf{q}_1 + \mathbf{q}_2)$. Third, the phase-matching condition in Eq. (1.12) limits the spread along the $(\mathbf{q}_1 - \mathbf{q}_2)$ and $(\omega_1 - \omega_2)$ coordinates. The spread in the arrival time difference between the two down-converted photons is inversely proportional to the phase-matching bandwidth, i.e., the spread in the $(\omega_1 - \omega_2)$ coordinate. For type-I phase matching, the symmetry of the two-photon field under sign reversal of $(\omega_1 - \omega_2)$ implies that the average arrival time difference between the photons is zero. Finally, and maybe most importantly, the two photons are entangled because Eq. (1.11) does not factorize into two functions of the individual coordinates.

1.3.5 Klyshko picture

The Klyshko picture provides a very intuitive interpretation of spatial correlations between down-converted photons [48, 52, 71]. This interpretation follows one detected photon at $\mathbf{x}_1$ backwards in time to the generating crystal where is is converted into the second forward propagating photon via a virtual reflection at the (possibly curved) pump beam profile. The spatial profile of the coincidence rate $R_{\mathrm{cc}}(\mathbf{x}_1, \mathbf{x}_2)$ is now given by how well the two detectors "see each other" via this

* We note that the phase matching condition in Eq. (1.12) needs to be adjusted somewhat to properly describe type-II SPDC and quasi phase-matched processes. For type-II SPDC one must impose different functions $k_z(\mathbf{q}, \omega)$ for photon 1 and photon 2. For quasi phase-matched processes one must compensate the wave-vector mismatch with the poling period (see for example chapters 3 and 4).

reflecting path. The Klyshko picture is very convenient in use and will often provide a good first guess of what can be expected in two-photon coincidence experiments.

Nevertheless, the Klyshko picture has severe limitations as it does not involve aspects of phase matching. The phase-matching condition generally confines the angular spread of down-converted light and causes spectral and spatial aspects of the two-photon field to be correlated. The two-photon field in Eq. (1.11) can be adapted to a Klyshko-picture form by simply removing the sinc-function part, i.e.,

$$A(\mathbf{q}_1, \omega_1, \mathbf{q}_2, \omega_2; 0) \sim \delta[\omega_p - (\omega_1 + \omega_2)] E_p(\mathbf{q}_1 + \mathbf{q}_2; z = 0) \qquad \text{[Klyshko picture]}.$$

The Klyshko picture works well in the thin-crystal limit where $L \to 0$ in Eq. (1.11).

Phase-matching aspects are very important in this thesis. Therefore, the Klyshko picture is generally insufficient to understand our experimental results. In chapter 4, we utilize near-field aspects of the two-photon field, which result from the phase-matching condition. In chapter 5, the phase-matching condition limits the dimensionality of the entanglement and the size of the two-photon speckle spots. In chapter 6, we use type-II down-conversion where the allowed optical detection bandwidth is drastically reduced by the phase-matching condition as compared to type-I phase matching. Chapter 3 is entirely devoted to a detailed investigation of the phase-matching condition in our crystals.

1.4 Thesis outline

This thesis contains four published papers (chapters 2-5) and one yet unpublished work (chapter 6) on two-photon interference. All works can be read independently. You might wish to read only a few of them. Below, we have provided a catchy description of each chapter to facilitate your choice.

- **Chapter 2:** It is well known that light can carry orbital angular momentum. The down-converted photons in SPDC light are entangled via their orbital angular momentum. If one of the photons is detected with orbital angular momentum $+l\hbar$ then the other collapses into $-l\hbar$ since the total amount of orbital angular momentum is conserved in the down-conversion process. **In chapter 2, we experimentally determine the Schmidt coefficients of the OAM eigenstates via two-photon interference**.

- **Chapter 3: This chapter contains a thorough characterization of SPDC and second harmonic generation (SHG) in periodically poled $KTiOPO_4$.** The investigated spatial aspects of the phase-matching condition are essential for the two-photon field used in chapters 4-6. As a bonus, we discovered how the observed phase-matching rings in SPDC light contain quantitative information on the quality of the poling structure in the nonlinear crystal.

- **Chapter 4:** Finally, more than 200 years after Young's double-slit experiment, **we present a complete and comprehensive description of the double-slit experiment for the two-photon case**. Two-photon interference allows for a wide variety of different fringe patterns. We are the first to measure them all and with unprecedented quality (see cover of printed thesis). Our results are backed-up by our simple comprehensive model for two-photon double-slit fringe patterns. Special attention is paid to the two-photon phase front, an important aspect that has often been overlooked. To generate these patterns, we utilize phase-sensitive properties of the two-photon field in both the near-field and far-field of the non-linear crystal.

- **Chapter 5:** Wave propagation in random media has intrigued and occupied many physicists in the last five decades. The most prominent feature of a multiply scattered wave is its random interference pattern called speckle. We wondered what two-photon speckle patters with spatial entanglement would look like. **In chapter 5 we present the first observation of two-photon speckle patterns**. We have found out how the spatial structure within two-photon speckle patterns is related to the structure of the scattering medium. Spatial entanglement gives two-photon speckle a much richer structure than ordinary one-photon speckle.

- **Chapter 6:** Only a few exotic one-photon interference phenomena are known to survive averaging over different realizations of disorder. Examples are enhanced backscattering and Anderson localization of light. Read chapter 6 for a sneak preview in yet unpublished work on **the first observation of a two-photon interference phenomenon that survives averaging over different realizations of disorder**.